Deep-space to Ground Laser Communications in a Cloudy World

Gary S. Wojcik*, Heather L. Szymczak, Randall J. Alliss, Robert P. Link,
Mary Ellen Craddock, Michael L. Mason

Atmospheric Effects Group, Information Technology Sector
TASC/Northrop Grumman Corporation, 4801 Stonecroft Blvd. Chantilly, VA 20151;

ABSTRACT

Future deep-space communications will require the collection and transmission of data from high-bandwidth links. NASA's Jet Propulsion Laboratory (JPL) is investigating the utility of laser communications for future missions to Mars and for future communication stations on the moon. Cloud cover impacts the availability of space to ground optical communications. Mitigating these impacts requires a geographically diverse network of ground communication. Selecting the number and location of stations for a network requires an optimization algorithm that can distinguish and rank site availability based on multi-year cloud climatologies for many locations around the globe. The optimization algorithm must also consider the movement and location of a space-borne probe. In this JPL-funded study, the TASC Lasercom Network Optimization Tool (LNOT) is used to determine optimal networks of receiving stations by analyzing cloud mask data from the continental United States, Hawaii, South America, Europe, northern and southern Africa, the Middle East, central and eastern Asia, and Australia. To generate cloud masks, raw visible and infrared radiance data from GOES (Geostationary Operational Environmental Satellite) and Meteosat satellites are compared to predicted clear sky background values. Several threshold tests in the Cloud Mask Generator (CMG) involving radiance-derived cloud identification tools (e.g., fog product, albedo product) are used to estimate the probability of cloud cover for a given pixel of a satellite image. When stations are chosen from a list of sites of interest, six stations are needed to achieve a network availability of 90 % or better.

Keywords: Laser communication, deep-space communications, cloud climatology, optimization process, ground station network, satellites, cloud detection

1. INTRODUCTION

The NASA Jet Propulsion Laboratory (JPL) is investigating strategies to support high availability laser communications for future missions to Mars and for communicating with future stations on the moon. Such projects will generate an ever increasing amount of data that must be transferred to ground locations. As an alternative to the current use of radio communications, deep-space to ground laser communications will provide a higher band-width to transfer these data with smaller power mass and power consumption subsystems. However, optical communications may be interrupted by cloud cover. Therefore, a mitigation strategy ensuring a high likelihood of a cloud-free line of site (CFLOS) between a ground station and the spacecraft or probe is needed to maximize the transfer of data. One strategy to address this problem is the use of "ground station diversity" in which several stations are "available" to receive communications should one or more sites be cloud covered or unreachable. For our purposes, we define "availability" to be the fraction of time that at least one station in the network has CFLOS and has a communication link with a probe, which must be at an elevation angle of 20^{o} or more. In this paper, we present our methodology for determining the minimum number of stations required to generate a network availability of at least 90 %, as specified by JPL. We also discuss the preliminary results of several optimal networks as selected through this methodology.

The availability of a communication link between a probe and a ground station network depends on many factors including the number and location of the sites in the network and the orbit of the spacecraft, which determines its elevation angle and the path length of transmission through the atmosphere. Typical meteorological patterns cause the cloud cover state at stations within a few hundred kilometers to be correlated. Consequently, stations within the network should be placed far enough apart to diminish these correlations. This requirement may lead to the selection of

*gary.wojcik@ngc.com; phone 1 703 633 8300 x7078; fax 1 703 449 3400

Free-Space Laser Communications V, edited by David G. Voelz, Jennifer C. Ricklin, Proc. of SPIE Vol. 5892
(SPIE, Bellingham, WA, 2005) · 0277-786X/05/$15 · doi: 10.1117/12.615435

a station that has a lower CFLOS than sites not selected but is less correlated with other network sites. The stations also need to be close enough to each other to produce a continuous communication link with the probe as the probe's position with respect to the ground changes with time.

At low elevation angles, increased air mass in the line of site may significantly scatter the transferred beams resulting in loss of data. Therefore, reliable communications may not be possible if the elevation angle is below a critical value, taken to be 20^{o} for this study as specified by JPL. Similarly, during the day, the brightness of the background sky may also affect optical communications. To lessen the effect of scattering, eligible stations need to be located at high altitudes. In different scenarios in this study, we allow stations at minimum altitudes of 0 km, 1 km, and 2 km to be considered for inclusion in the networks. Also, 30 sites of interest from around the globe selected by JPL are studied (Fig. 1; Table 1). These locations currently contain some of the infrastructure needed for a deep-space communication ground station (e.g., observatory, telescope, etc.). Note that no agreements to use any of the sites that are not currently accessed by JPL have been established.

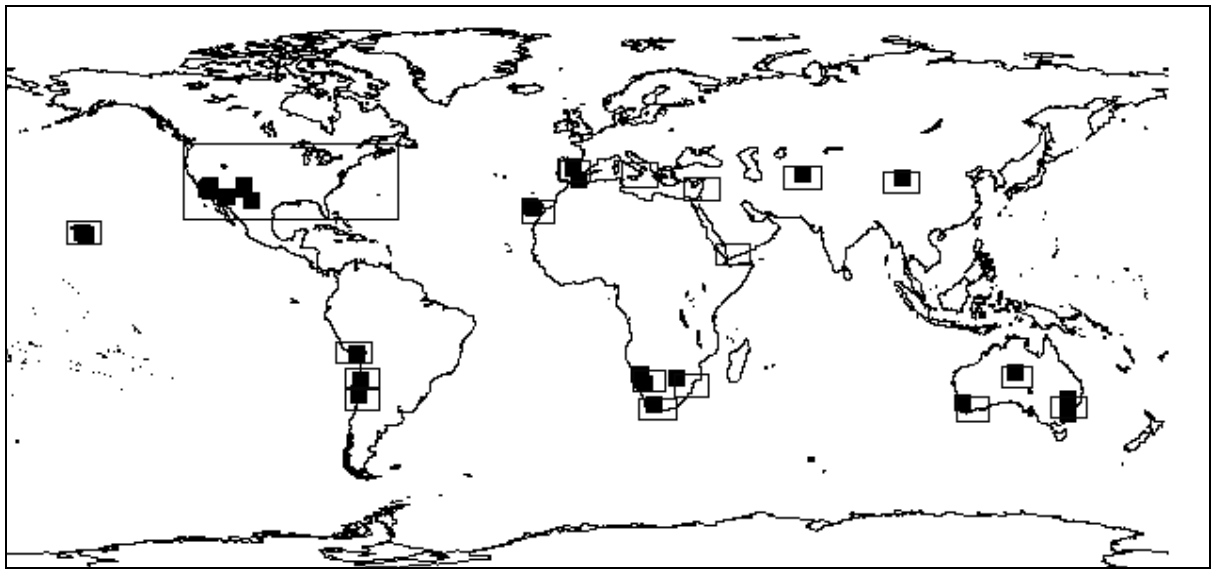

Figure 1: Regions enclosed within the black rectangular boxes are those examined in this study. Solid black squares indicate the location of the sites of interest used in the LNOT Restricted runs. See Table 1 for the site names and locations. Note that the squares for two or more of these sites may overlap.

The selection of a network of sites requires an optimization scheme that can distinguish and rank site availability based on a multi-year cloud climatology for many locations around the globe and based on the movement and location of the probe. Previous studies have focused on limited domains in the continental United States (CONUS), Hawaii, and South America[1, 2]. Networks derived from these limited domains have their availabilities penalized for the times when the probe is below the horizon (i.e., no communication link). Therefore, in this study, cloud mask data from selected regions in CONUS, Hawaii, South America, Europe, northern and southern Africa, the Middle East, central and eastern Asia, and Australia (Fig. 1) are analyzed with the TASC Lasercom Network Optimization Tool (LNOT). LNOT is in-house software that applies optimization algorithms to the cloud mask data and probe location to determine networks of stations with optimal availabilities. By expanding the domain of interest to include regions around the world, the probe is more frequently visible to at least one station in the network, increasing the availabilities.

Cloud masks, two-dimensional projections of clouds on the surface that show the horizontal location of clouds as seen from a satellite, have been created with the Cloud Mask Generator (CMG). CMG uses several threshold tests involving the radiance-derived cloud identification tools (i.e., fog product, albedo product) collected from the Geostationary Operational Environmental Satellite (GOES) and European Organization for the Exploitation of Meteorological Satellites (EUMETSAT) Meteosat satellites to calculate the likelihood of cloud cover in a given satellite pixel.

Table 1: The names and locations of the sites of interest indicated in Fig. 1.

Goldstone NASA Deep Space Network, CA USA	Teide, Canary Islands
Mount Wilson, CA USA	Madrid NASA Deep Space Network, Spain
Palomar, CA USA	Calar Alto, Spain
Table Mountain, CA USA	Gamsberg Table Mountain, Namibia
Kitt Peak, AZ USA	H.E.S.S. Telescope, Namibia
White Sands, NM USA	Solar Smithsonian, Namibia
Starfire Optical Range, NM USA	South Africa Astron Telescope, South Africa
McDonald Observatory, TX USA	Hartebeesthoek, South Africa
Mauna Kea, HI USA	Purple Mountain Observatory, China
Mount Haleakala, HI USA	Perth Observatory, Australia
Arequipa, Peru	Alice Springs, Australia
La Silla, Chile	Mount Stromlo, Australia
Paranal Chile	Anglo/Aust Telescope Facility, Australia
Las Campanas, Chile	Canberra DSN, Australia
La Palma, Canary Islands	Shokin Majdanak Observatory, Uzbekistan

In section 2, we present information on the cloud data collected from GOES and Meteosat satellites and we explain the cloud detection algorithms used by the CMG to develop cloud masks. We discuss the optimization process in LNOT, which is used to select optimal networks of stations, in section 3. Preliminary results of availabilities for ground station networks determined with the optimization process on the cloud mask data are presented in section 4. This work is summarized in section 5.

2. CLOUD ANALYSIS

2.1. Satellite data

The analysis period presented here extends from June 2003 through May 2004. Note that our database of satellite images for CONUS and Hawaii stretches from 1997 to present, while the database for the other regions (Fig. 1) contains data from 2003 to present. The data for regions in the western part of CONUS and Hawaii are from GOES-West, while the data for South America and the eastern part of CONUS come from GOES-East. GOES-9 provided the data for the Australia and China regions. Data for regions in Europe and Africa are from Meteosat-7, while those for the Middle East and central Asia regions are from Meteosat-5. For the period of interest, satellite data for CONUS and Hawaii are at 15 min resolution while the resolution for the South America, Europe, and Africa regions is 30 min. The China, Australia, and Middle East regions have satellite data every hour.

GOES imagers have five bands: visible (0.6 μm), shortwave infrared (SWIR; 3.9μm), water vapor (6.7 μm), longwave infrared (LWIR; 10.7 μm), and split window (11.2 μm). We replaced the water vapor channel, which is not used for cloud detection, with the reflectivity product during the day and the fog product at night (see below and section 2.3 for more detail on these products). The spatial resolution of the visible band is 1 km and that for the other bands is 4 km. For our purposes, the 1 km data is resampled to 4 km resolution so that it is comparable to the other bands.

During the day, Meteosat imagers provide data in only two spectral bands (visible (0.5-0.7 μm) and the LWIR (10.5-12.5 μm) and just one (LWIR) during the night. The spatial resolution is 5 km. The lack of data channels from the Meteosat satellites, in particular, the lack of the SWIR at night, reduces the accuracy of the generated cloud masks. The SWIR is used to calculate the reflectivity product and the fog product. The reflectivity product helps to

differentiate between clouds and snow cover during the day and the fog product aids in the detection of fog and low and high clouds at night. With no SWIR data from the Meteosat satellites, these products cannot be generated and the quality of the cloud analysis is reduced. See section 2.3 for more information.

2.2. Clear Sky Background

Our cloud analysis techniques for the GOES data are described in detail by Alliss et al.[3]. All cloud tests consist of comparing satellite image values to dynamically computed clear sky background (CSB) values pixel by pixel in the regions of interest. The CSB is discussed below and main cloud test algorithms (albedo, LWIR, fog, and reflectivity) are discussed in section 2.3.

The CSB is defined as the amount of radiation emitted and/or reflected from a surface that reaches a satellite sensor when no clouds are present. The CSB varies spatially and temporally and is influenced by the radiative properties of the surface material, surface temperature, terrain height, soil moisture, and solar illumination angle. Because of these variations, the CSB must be calculated for each region separately, on a pixel by pixel basis, as a function of the above-mentioned factors to generate accurate cloud masks. For example, if the albedo test used a fixed threshold for typical differences between the observed and calculated CSB albedos for all locations, then false cloud detections would be likely over naturally highly reflective regions such as White Sands, NM or the salt flats of northern Chile.

Four CSBs are estimated in the CMG: albedo, reflectivity, LWIR, and fog[1]. The CSB is calculated for each pixel by using data from clear times over the previous 30 days at a given analysis time (e.g., 1400 GMT). This approach provides sufficient clear sky data and reduces the effect of diurnal and seasonal cycles of temperature and illumination, in particular, on the calculated CSB. The database from which clear times are determined includes not only the satellite imagery, but also ancillary surface and ship observations collected by the National Weather Service (NWS), World Meteorological Organization (WMO), and at several telescope observatories in South America.

The albedo CSB is calculated by identifying the darkest 10 % of albedo values from the previous 30 days of visible images. The selected albedo values are averaged to define the CSB for each pixel. The reflectivity CSB is determined only during the day and when snow cover is not likely present. Like the albedo, the darkest 10 % reflectivity product values from the previous 30 days are selected and averaged to generate the CSB.

To develop the fog product CSB, the warmest 10 % of LWIR values for the pixel over the previous 30 days are selected. The corresponding fog product values are then averaged to give the fog CSB. Note that the procedure used to generate the fog product CSB differs from that used to generate the albedo and reflectivity products in which clear pixels are chosen based on the albedo and reflectivity values themselves. Both fog product extremes indicate clouds and the selection of the 10 % warmest or coldest values will not provide the needed information; therefore, the two-step process is used for the fog product CSB.

The LWIR CSB is determined as the average of the difference between the LWIR temperature from the satellite for a given pixel and the LWIR CSB temperature estimated from a linear regression model. The regression model is developed with data from clear sky pixels that are used as prototypes. These prototype pixels are selected by a series of tests that find pixels with a high probability of being clear, even without the benefit of any of the cloud tests. The coefficients of the regression model for twelve predictors are fit with the data from the prototype pixels. The predictors include satellite data, time, terrain, and regional observations such as cloud cover and air temperature from the NWS and WMO.

The LWIR regression model estimates the clear sky LWIR brightness temperature for each pixel. The LWIR residuals are the differences between the regression model temperatures and the measured imager LWIR temperatures. The warmest 10 % of the LWIR residuals are averaged to determine the LWIR residual CSB that is used in the LWIR cloud tests.

2.3 Cloud Tests

The CSB values and the satellite data are compared in four main cloud tests in the CMG: the LWIR test, the albedo product test, the fog product test, and the reflectivity product test. The LWIR test is applied at all times of the day, unlike the albedo, reflectivity, or fog product tests. A pixel is considered to be cloudy if the LWIR CSB for a given pixel exceeds the LWIR from the satellite by the threshold value or greater. This test cannot easily detect fog/low clouds at night because the cloud top temperatures are very similar to the surface temperatures. It is unlikely that clouds will radiate in the LWIR at temperatures greater than 300K. A pixel is deemed clear if the LWIR temperature is greater than 300K, even if the LWIR cloud test indicates that it is cloudy.

As mentioned above, the detection of fog and low stratus clouds at night is difficult with the LWIR. The fog product test is a multi-spectral test that compares values of the fog product calculated as the difference between the LWIR and the SWIR brightness temperatures[4]. The temperature differences result mainly because clouds observed in the SWIR have an emissivity that is 20%-40% lower than clouds observed in the LWIR[5]. Therefore, at night, liquid stratiform (low) clouds appear colder in the SWIR than they do in the LWIR. Typical T_{LWIR}-T_{SWIR} for fog and low stratus are approximately 2 K or larger[6]. The fog product can also detect ice clouds, which are highly transmissive and therefore appear warmer in the SWIR. Typical values for ice clouds are T_{LWIR}-T_{SWIR} are approximately -5 K or lower[6]. The daytime SWIR is dominated by reflected solar SWIR and therefore, the fog product is only useful at night.

The albedo test, which uses visible data, is applied when the solar zenith angle is below 89^{o}. This test will detect clouds if the pixel is more reflective than the albedo CSB and the difference is greater than a predefined threshold for that pixel. If the difference between the calculated albedo and the CSB is less than the threshold, the pixel is deemed clear. The albedo test may falsely detect snow as clouds.

The shortwave reflectivity product is implemented during the day to decide if a pixel is cloudy or if the surface is snow-covered. This product indicates the amount of reflected solar SWIR detected and is derived by removing the thermal component from the SWIR[7,8]. Water clouds are highly reflective in the SWIR while ice clouds are poorly reflective in the SWIR. As a result, water clouds appear as bright white and poorly reflective ice clouds and snow appear as dark gray or black in the resulting images. The reflectivity product, then, can easily distinguish between low clouds and snow cover. The reflectivity test is only applied when and where snow cover is likely and can override a false cloud detection for snow cover indicated by the albedo test. To ensure that high ice clouds (which also appear dark in the reflectivity test) are not present, the LWIR test must not indicate the presence of high clouds for a pixel to be considered clear.

Meteosat-5 and Meteosat-7 provide only LWIR data at night and only visible and LWIR data during the day. The lack of a SWIR band from these two satellites limits the accuracy of the cloud mask. At night, with no SWIR, there is no fog product with which to detect low clouds or fog. During the day, there is no reflectivity product and so it is possible that false detection of snow as clouds from the albedo test may occur, resulting in less accurate cloud masks.

With the CSB and satellite data, the CMG performs the necessary tests to determine the cloud masks. During the day, for example over southern Italy and Sicily (Fig. 2), the LWIR and albedo products are used to detect clouds with the resulting mask accurately showing the location of clouds. At night when low clouds cannot be adequately detected by the LWIR, the fog product is vital to developing accurate cloud masks. In fact, in a cloud scene from southwestern Australia (Fig. 3), the low clouds over the land would not have been detected without the fog product.

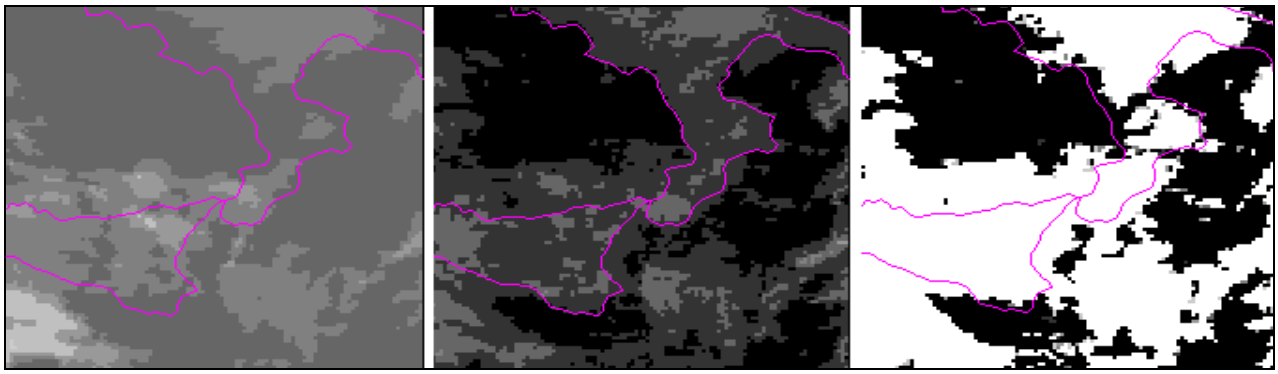

Figure 2: A sample cloud scene during the day for southern Italy and Sicily. The image on the left is the LWIR image from Meteosat-7 during the day. The image in the center is the corresponding visible image from Meteosat-7. For these two images, the lighter grey images indicate clouds. The cloud mask on the right shows clouds as white and was generated with the CMG.

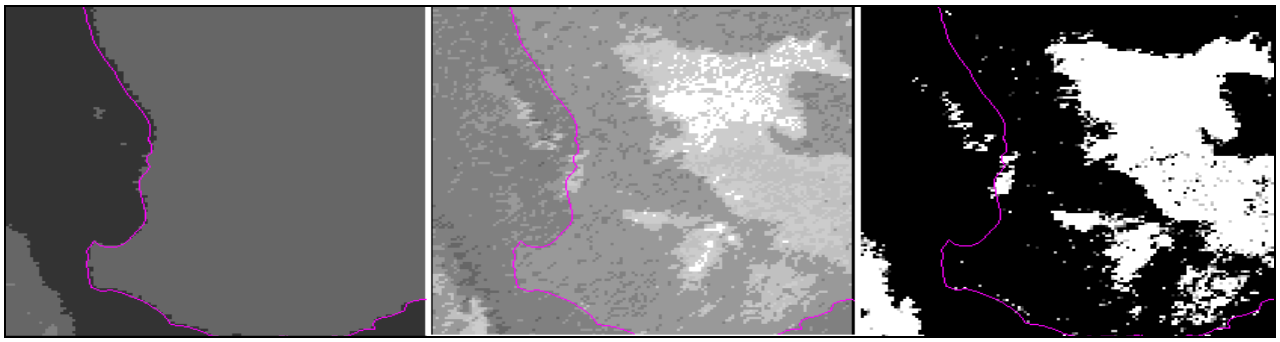

Figure 3: A sample cloud scene during the night for southwestern Australia. The image on the left is the LWIR image from GOES-9. Note the small area of clouds in the southwestern corner over the water. The image in the center is the corresponding fog product calculated from data provided by GOES-9. Note the large area of fog in the lighter grey and white shades over the land. The cloud mask on the right shows clouds as white and was generated with the CMG.

3. NETWORK OPTIMIZATION AND EVALUATION

The goal of optimization in developing a network of ground stations for optical communications is to achieve the highest availability for the network, i.e., the greatest percentage of time during which at least one ground station can communicate with the probe, with the fewest number of stations in the network. Not only must the cloud fractions at each site be considered, but also their location with respect to one another must be considered. Selecting stations with very low cloud fractions all in the same area, say within several hundred kilometers of one another, will result in low availabilities. In such a case, the low availability results because the stations could not see the probe a large percentage of the time because of the probe's movement with respect to the earth. If stations whose cloud patterns are highly correlated are selected, the availability may also be reduced because when one station is cloudy and thus unavailable, one or more of the other stations is likely to be the same. However, widely separated ("geographically diverse") stations will tend to be less correlated and because they would be positioned over a wide region of the globe, availability would be expected to be higher than the scenarios outlined above.

The process of finding an optimal ground station network is a discrete optimization problem. With over 420,000 pixels in our cloud database for the regions considered in this study, the search space must be reduced to be practical. JPL provides some constraints on the locations of the stations such as they must be within ±41° latitude; elevation angle of the probe with respect to the station must be greater than 20° for each pixel to be considered; minimum station altitude of 2 km (we also do tests for 0 km and 1 km); or the sites must be selected from a list of sites of interest. Even with these constraints, the database is too large to search exhaustively for the network with the maximum availability. Therefore, the optimization algorithm must be able to find the desired networks by searching only a small fraction of the network configuration space.

The optimization process we employ will seek a balance between what we call "locality" and "robustness". Locality refers to the idea that good network configurations are close together in space. This feature lets the algorithm make progress in selecting stations. If we did not have the locality feature, the n^{th} guess would be no better than the first guess. On the other hand, it is desirable that the algorithm not get trapped in local extrema in the configuration space. This feature is known as robustness. Our optimization process represents a tradeoff between locality and robustness in two distinct stages. In the first stage, the algorithm searches widely over the entire configuration space, sacrificing some locality in favor of robustness. Once the algorithm arrives in the vicinity of the solution, the second stage begins. In the second stage, some robustness is sacrificed in favor of locality as the algorithm finds the best configuration in the neighborhood of the last configuration found by the first stage. The limited robustness found in the second stage is not of concern because we assume that the optimal solution is nearby when we begin the second stage.

A typical optimization run evaluates more than 40 million networks. At the end of the optimization process, we further evaluate the availability of the ten best networks found by considering detailed line of sight calculations that take into account ground station locations, effects of parallax between the GOES imager and the probe, the elevation angle of the probe, and the cloud amount in a 2400 km^2 area centered on each station. To make these calculations, the position of the probe with time must be known. We assume that the probe is at 0^o inclination to the ecliptic, with a radius of 1.5237 AU (Astronomical Units; 1 AU= 149,597,870 km). This orbit is similar to that for Mars and is much faster to calculate than an elliptical, inclined orbit. Along with availabilities, we calculate complete network status at every 15 min time step, intra-network correlations, serial correlations, and outage distributions.

We present results for two different categories of optimization experiments. First, the LNOT optimization process selects networks ranging from two to six stations from any of the pixels representing land in the regions shown in Fig. 1 for minimum altitudes of 0 km, 1 km, and 2 km. These results are referred to as "Unrestricted". For "Restricted" site results, the optimization algorithms select stations from only those listed in Table 1 and shown in Fig. 1.

4. PRELIMINARY RESULTS

To achieve an availability of 90 % or greater with the Restricted runs, six sites are necessary (Fig. 4). The availability of this network from June 2003 through May 2004 is 91 %. The stations are distributed around the globe with one in CONUS, one in South America, one in southern Africa, and three in Australia. Such a distribution would be expected to achieve the greatest amount of time that at least one site in the network has a communication link. For the top ten networks as determined by LNOT, the distribution of sites by region is exactly the same. However, other stations like Palomar, La Silla, HESS Telescope, Gamsberg Table Mountain, and Anglo/Aust Telescope, are also found in the other networks, all of which have an availability of greater than 90 %. These results suggest that there is some flexibility in the placement of ground stations without unduly influencing the overall availability. For the best six site network, the monthly availability ranges from 88 % in June to 98 % in February (Fig. 5). Recall that the optimal network and the availability are based on a probe in approximate Mars orbit. If the probe is sent to a different deep-space destination, the networks and availabilities will be different.

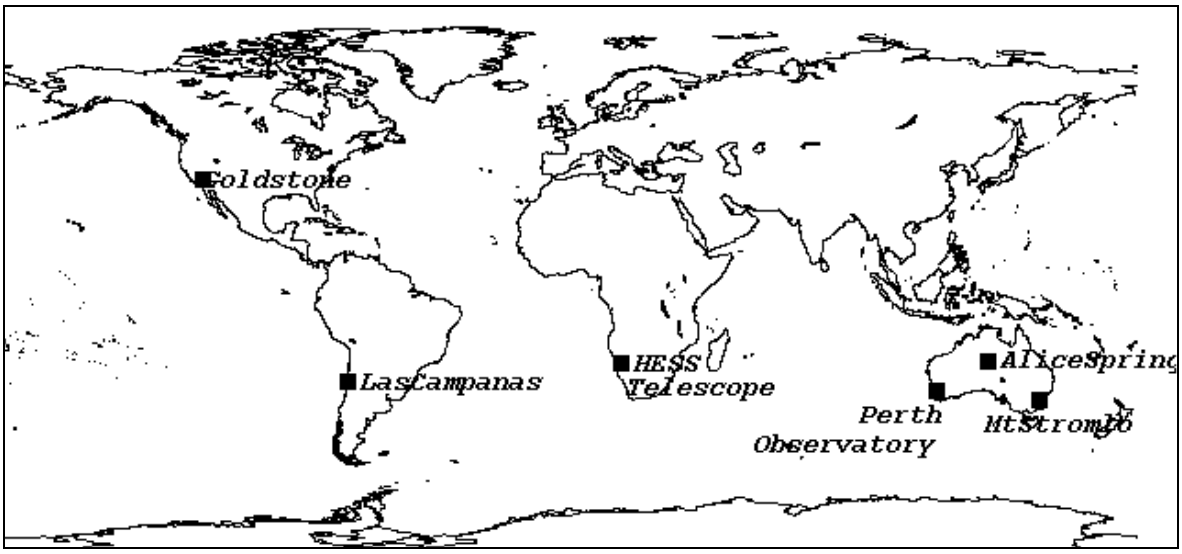

Figure 4: Locations of the stations in the best six site network as computed by LNOT for the Restricted runs. The availability for this network for June 2003 – May 2004 was 91 %.

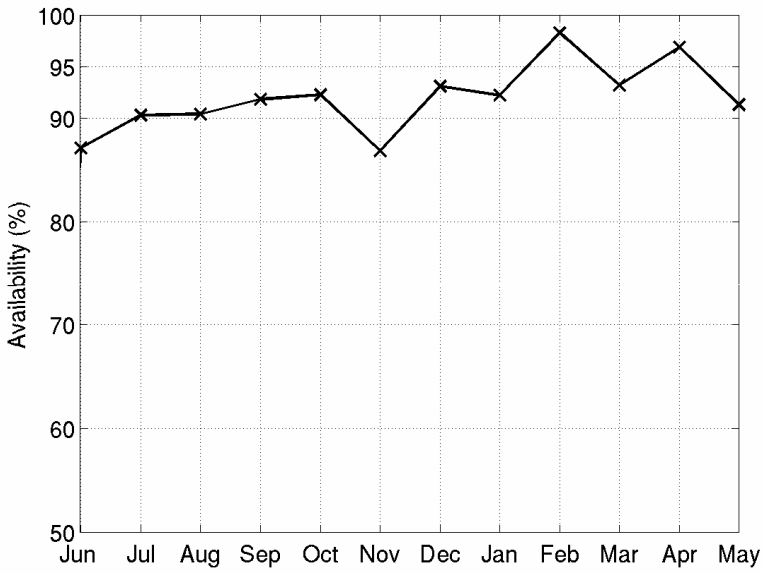

Figure 5: Month by month availability for the best six site network calculated by LNOT for the Restricted runs for June 2003 through May 2004.

No sites from Europe, Canary Islands, or Asia were selected for this period. The reason for this is that the probe was in its southern declination phase over the period of our data (Fig. 6). When the probe is in this position, stations in the southern hemisphere have better coverage or a larger likelihood of establishing a communication link with the probe (assuming clear skies). The probe had just begun its northern declination phase by May 2004. When another year is added to our database, the optimization process will consider both declination phases of the probe, perhaps increasing the likelihood of the northern hemisphere sites being selected for the networks. Moreover, optimizing over a longer time period will necessarily change the ground stations selected and the availabilities of the new networks.

Note that two, three, four, and five site networks give availabilities of 54 %, 75 %, 82 %, and 89 %, respectively. Given the uncertainty of our calculations, it is possible that a five site network can also produce a satisfactory availability.

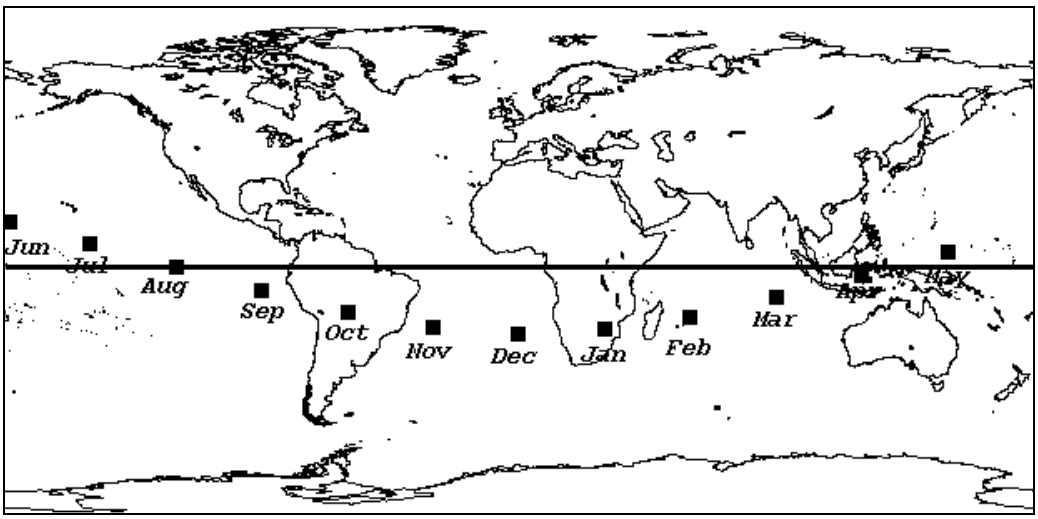

Figure 6: Black squares indicate the latitude of the probe on the last day of each month for the period of June 2003 through May 2004. The equator is indicated by the solid horizontal black line through the center of the figure.

For the Unrestricted runs allowing stations with a minimum altitude of 0 km, a five site network is sufficient to attain a 90 % availability, while at 1 km a six site network is needed (Fig. 7). Because the optimal six site network with a minimum altitude of 2 km has an availability of 83 %, we will need to generate networks with more than six stations to determine a network with an availability of 90 % or above for these conditions. As the minimum allowable altitude increases, the number of locations from which to choose from decreases, resulting in lower availabilities. In addition, the best six site network at 2 km has all but one of its stations in the northern hemisphere (Fig. 8), in contrast to the results of the best Restricted network (Fig. 4). Those parts of Africa and Australia that are considered in this study contain little territory above 2 km so locations in these areas are not selected in the best networks.

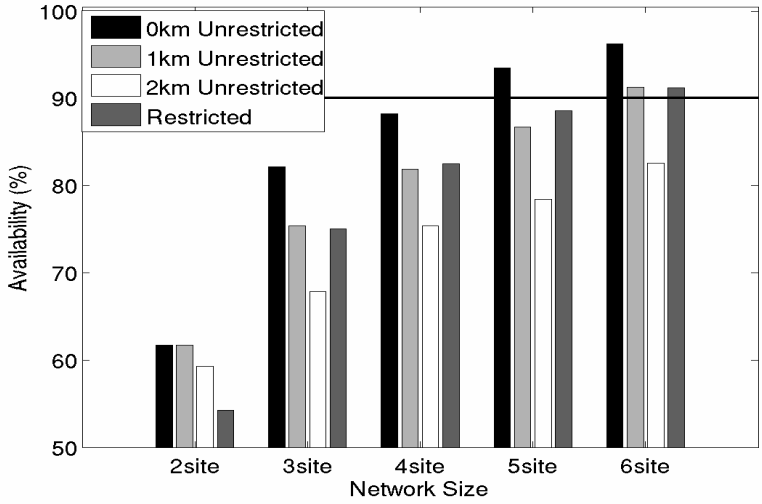

Figure 7: Availabilities for the Unrestricted and Restricted networks for June 2003 through May 2004 for networks of two, three, four, five and six sites.

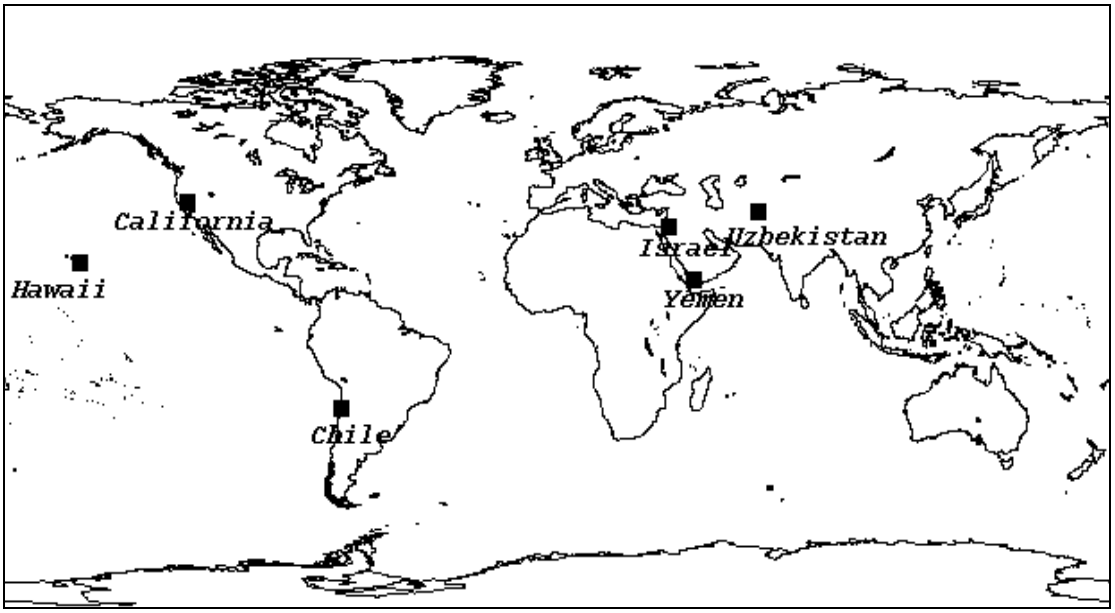

Figure 8: Locations of the stations in the best six site network with a 2 km minimum altitude as computed by LNOT for the Unrestricted runs. The availability for this network for June 2003 – May 2004 was 83 %.

5. Summary

Laser communications between ground stations and space-borne probes can be interrupted by clouds. To mitigate the effect of clouds and to attain a high availability of the communication link between the ground and the probe, a geographically diverse network of ground stations is needed. The stations in this network should have limited correlation with one another and should be placed so that there is overlap between stations as the probe rises and sets every day. With such a network, if one station is cloudy or does not have coverage of the probe, another station can be used in its place.

The determination of these ground station networks requires cloud climatologies and an optimization algorithm that considers cloud cover and the position of a probe with respect to the ground stations. LNOT, in-house software that selects networks of stations with optimal availabilities, has been applied to the problem of finding a network that can communicate with a probe in an approximate Mars orbit with an availability of 90 % or greater. The regions of interest for which we have begun developing cloud climatologies are CONUS, Hawaii, South America, Europe, Africa, the Middle East, central and eastern Asia, and Australia. When selecting stations from a list of sites of interest (those which already contain significant infrastructure) from these regions, an availability of 90 % or greater is attained with a network of six stations. When the sites are selected from all available locations at or above 2 km, a six stations network gives an availability of 83 %. Larger network sizes will have to be considered to meet the availability goal of 90 % or above.

The results presented here are for the period of June 2003 through May 2004 and should be considered only preliminary. They do, however, suggest that a ground station network with an availability of at least 90 % for laser communications is feasible. A long term cloud database will allow the network to be selected with knowledge of monthly and yearly meteorological variations. Also, with more years of data, the probe will be located at more northern declinations at times, increasing the importance of northern hemisphere stations in networks. In addition, the results presented here reflect a probe in an approximate Mars orbit. Whether the optimization is done for additional years of

data or for a different mission such as to the moon, Jupiter, or other deep-space destinations, the optimal ground station networks and availabilities will be different from those shown here.

ACKNOWLEDGEMENTS

The authors would like to thank Dr. Sabino Piazzolla and Dr. Keith Wilson of NASA-JPL for their feedback and discussion during this research. This research is funded by the Jet Propulsion Laboratory, California Institute of Technology, under contract with the National Aeronautics and Space Administration.

REFERENCES

1. R. J. Alliss, R. L. Link, M. E. Craddock, "Mitigating the impact of clouds on optical communications," in *13th Conference on Satellite Meteorology and Oceanography*, American Meteorological Soc., September 2004.
2. R.L. Link, M. E. Craddock, and R. J. Alliss, "Mitigating the impact of clouds on optical communications," in *2005 IEEE Aerospace Conference*, IEEE Aerospace, March 2005.
3. R. J. Alliss, M. E. Loftus, D. Apling, and J. Lefever, "The development of cloud retrieval algorithms applied to goes digital data," in *10th Conference on Satellite Meteorology and Oceanography*, pp. 330–333, American Meteorological Soc., January 2000.
4. G. P. Ellrod, "Advances in the detection and analysis of fog at night using goes multispectral infrared imagery," *Weather Forecasting,* **10**, pp. 606–619, 1995.
5. G. E. Hunt, Radiative properties of terrestrial clouds at visible and infrared thermal window wavelengths," *Quarterly Journal of the Royal Meteorological Society*, **99**, 346-359.
6. T. F. Lee, F. J. Turk, and K. Richardson, "Stratus and fog products using GOES-8 3.9 μm data," *Weather Forecasting,* **12**, pp. 664–677, 1997.
7. R. C. Allen, Jr., P. A. Durkee, and C. H. Wash, "Snow/cloud discrimination with multispectral satellite measurements," *Journal of Applied Meteorology,* **29**, pp. 994–1004, 1990.
8. M. Setvak and C. A. Doswell, III, "The AVHRR channel 3 cloud top reflectivity of convective storms," *Monthly Weather Review,* **119**, pp. 841–847, 1991.